Dalton Transactions

Dynamic Article Links

Cite this: *Dalton Trans.*, 2011, **40**, 5895

www.rsc.org/dalton

PAPER

Interaction of Triapine and related thiosemicarbazones with iron(III)/(II) and gallium(III): a comparative solution equilibrium study†

Éva A. Enyedy,*[a] Michael F. Primik,[b] Christian R. Kowol,[b] Vladimir B. Arion,[b] Tamás Kiss[a,c] and Bernhard K. Keppler[b]

Received 27th December 2010, Accepted 22nd March 2011
DOI: 10.1039/c0dt01835j

Stoichiometry and stability of Ga^{III}, Fe^{III}, Fe^{II} complexes of Triapine and five related α-*N* heterocyclic thiosemicarbazones with potential antitumor activity have been determined by pH-potentiometry, UV-vis spectrophotometry, ^{1}H NMR spectroscopy, and spectrofluorimetry in aqueous solution (with 30% DMSO), together with the characterization of the proton dissociation processes. Additionally, the redox properties of the iron complexes were studied by cyclic voltammetry at various pH values. Formation of high stability *bis*-ligand complexes was found in all cases, which are predominant at physiological pH with Fe^{III}/Fe^{II}, whilst only at the acidic pH range with Ga^{III}. The results show that among the thiosemicarbazones with various substituents the N-terminal dimethylation does not exert a measurable effect on the redox potential, but has the highest impact on the stability of the complexes as well as the cytotoxicity, especially in the absence of a pyridine-NH_2 group in the molecule. In addition the fluorescence properties of the ligands in aqueous solution and their changes caused by Ga^{III} were studied.

Introduction

Thiosemicarbazones (TSCs) are extensively investigated as they exhibit anticancer, antibacterial, antiviral and other biological properties.[1] Especially α-*N*-heterocyclic TSCs with a nitrogen containing heterocycle in α position to the thiosemicarbazide side chain exert significant antitumor activity *in vitro* and *in vivo*. The proposed mechanism of action is based on their ability to inhibit the iron-requiring enzyme ribonucleotide reductase (RR), the rate determining enzyme in the supply of deoxyribonucleotides for DNA synthesis required for cell proliferation. Triapine (3-aminopyridine-2-carboxaldehyde thiosemicarbazone, 3-AP, see Scheme 1) is the most prominent representative among these compounds as it has been tested in a variety of tumor cell lines in the preclinical setting and is currently undergoing different phase I and II clinical trials.[2] Also di-2-pyridyl TSCs were found to be highly potent against melanoma, breast cancer and neuroepithelioma cells[3,4] and their anticancer activity was confirmed *in vivo* in several human xenografts in mice.[5]

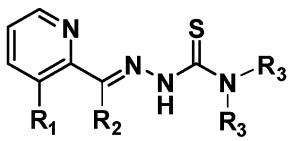

	R_1	R_2	R_3
Triapine	$-NH_2$	-H	-H
FTSC	-H	-H	-H
PTSC	-H	-H	$-CH_3$
APTSC	$-NH_2$	-H	$-CH_3$
FaTSC	-H	$-NH_2$	-H
AcTSC	-H	$-CH_3$	-H

Scheme 1 Ligands used in this study: **Triapine** = 3-aminopyridine-2-carboxaldehyde thiosemicarbazone; **FTSC** = 2-**f**ormylpyridine **t**hio**s**emi**c**arbazone; **PTSC** = **p**yridine-2-carboxaldehyde N^4,N^4-dimethyl-**t**hio**s**emi**c**arbazone; **APTSC** = 3-**a**mino**p**yridine-2-carboxaldehyde N^4,N^4-dimethyl**t**hio**s**emi**c**arbazone; **FaTSC** = 2-pyridine**f**orm**a**mide **t**hio**s**emi**c**arbazone; **AcTSC** = 2-**ac**etylpyridine **t**hio**s**emi**c**arbazone.

Compounds bearing the α-pyridyl TSC backbone are known to possess strong iron chelating properties.[6] It was suggested that the formation of an intracellular iron complex plays a crucial role in the mechanism of enzyme inhibition. The iron-TSC complexes have to be redox active to undergo redox-cycling and generate reactive oxygen species (ROS), which are able to quench the active site tyrosyl radical of the RR required for the enzymatic activity.[7] This mechanism is suggested to be at least partially

[a]*Department of Inorganic and Analytical Chemistry, University of Szeged, P.O. Box 440, H-6701, Szeged, Hungary. E-mail: enyedy@chem.u-szeged.hu; Fax: +36 62 420505*
[b]*University of Vienna, Institute of Inorganic Chemistry, Währinger Strasse 42, A-1090, Vienna, Austria*
[c]*Bioinorganic Chemistry Research Group of the Hungarian Academy of Sciences, University of Szeged, P.O. Box 440, Szeged, H-6701, Hungary*

† Electronic supplementary information (ESI) available: Additional concentration distribution curves, UV-vis absorption, ^{1}H NMR, fluorescence (3D) emission and ESI-MS spectra with some cytotoxicity data. See DOI: 10.1039/c0dt01835j

responsible for the antiproliferative activity of TSCs. As a result, the coordination chemistry of Fe^{II} and Fe^{III} complexes of TSCs has been receiving considerable attention, nowadays. Coordination of TSCs to iron occurs usually *via* tridentate ($N(pyr),N^1,S^-$) binding.[6–9] This arrangement of the donor atoms is also suitable for coordination to other transition metal ions, *e.g.* Cu^{II}, Zn^{II}, Ru^{III}, Pd^{II} and Ga^{III}, which can result in complexes with higher cytotoxicity than that of the metal-free ligand alone.[10–13]

In our previous work a series of Fe^{III} and Ga^{III} complexes of some derivatives of Triapine was synthesized and studied for their antitumor potency together with that of the metal-free ligands.[8] These investigations showed that the dimethylation of the terminal nitrogen (N^4) strongly enhances the cytotoxicity of the TSCs and that of their Fe^{III} and Ga^{III} complexes. However, this increase can only be observed in the absence of any NH_2 group in the molecule. The characterization of the complexes was performed in solid phase or in solution of organic solvents. However, the knowledge of the speciation and the most plausible chemical forms of these complexes in *aqueous* solution at physiological pH is a mandatory prerequisite for understanding the alterations in the efficacy of the complexes formed with Triapine and its derivatives and may be useful for the design of more effective chemotherapeutics. Quite little information is available in the literature about the thermodynamic stability of these complexes. In particular, although it is thought that the iron complex of Triapine is the active species inside the cells the stability constants of Fe^{III} have not been reported so far and no data for Ga^{III}-TSC complexes are available.

Therefore, detailed pH-potentiometric, UV-vis spectrophotometric, ^1H NMR spectroscopic and spectrofluorimetric measurements have been performed to investigate the stoichiometry and stability of Fe^{III} and Ga^{III} complexes formed with Triapine, 2-acetylpyridine thiosemicarbazone (AcTSC), 2-pyridineformamide thiosemicarbazone (FaTSC), 2-formylpyridine thiosemicarbazone (FTSC), and the N^4-dimethylated derivatives of Triapine (PTSC) and FTSC (APTSC) in a water/dimethyl sulfoxide (DMSO) mixture in addition to the proton dissociation processes of the ligands. Due to the importance of the redox behavior of the Fe^{III} complexes the formal redox potential values have been measured in aqueous solution at various pH values. In addition the solution equilibrium results for the Fe^{II} complexes of FTSC, FaTSC and AcTSC are reported here and the data are discussed in comparison with our recently published results for complexes of Triapine, PTSC and APTSC with Cu^{II}, Zn^{II} and Fe^{II}.[14]

Previously, it was shown that Triapine and its Zn^{II} complex possess intrinsic fluorescence allowing for the monitoring of the uptake and intracellular distribution in human cancer cells by fluorescence microscopy.[15] Therefore, herein also the pH dependent fluorescence properties of the TSC ligands as well as their corresponding Ga^{III} complexes are explored and presented.

Results and Discussion

Proton dissociation processes

The proton-dissociation processes of the TSCs (shown in Scheme 1) were followed by pH-potentiometry, UV-vis spectrophotometry and spectrofluorimetry as well as ^1H NMR titrations. All kinds of studies were performed in 30% (w/w) $DMSO/H_2O$ solvent mixture because of the poor solubility of the ligands in pure water, especially at higher concentrations necessary for pH-potentiometry. The hydrolytic stability of the ligands Triapine, PTSC and APTSC was monitored previously.[14] Titrations of FTSC, FaTSC and AcTSC also indicated that no ligand decomposition occurred in the pH range studied. Two proton-dissociation processes for the ligands FTSC, FaTSC and AcTSC could be determined by pH-potentiometry and UV-vis spectrophotometry and protonation constants are collected in Table 1 together with the previously published data for Triapine, PTSC and APTSC.[14] Constants obtained by the two different methods are in reasonably good agreement. pK_1 can presumably be attributed to deprotonation of the pyridinium unit and pK_2 to the deprotonation of the hydrazinic N^2–H group of the thiosemicarbazide moiety. In the latter the resulting negative charge is mainly localized on the S atom *via* the thione–thiol tautomeric equilibrium.[4,14] At physiological pH all compounds are charge neutral (in HL form) enabling an easier passage across the cell membrane than its protonated (H_2L^+) or deprotonated (L^-) form.

Table 1 Protonation and proton dissociation for the TSC ligands studied (t = 25.0 °C, I = 0.10 mol dm^{-3} (KCl) in 30% (w/w) $DMSO/H_2O$)[a]

	Triapine[b]	FTSC	PTSC[b]	APTSC[b]	FaTSC	AcTSC
$\log\beta([HL])$[c]	10.78	11.13(1)	10.54	10.29	11.61(1)	11.52(1)
$\log\beta([H_2L^+])$[c]	14.70	14.26(1)	13.92	14.60	14.76(1)	15.16(1)
$\log\beta([HL])$[d]	10.86	11.12(1)	10.52	10.35	11.64(1)	11.66(1)
$\log\beta([H_2L^+])$[d]	14.65	14.16(1)	13.81	14.60	14.69(2)	15.18(1)
pK_1[c]	3.92	3.13	3.38	4.31	3.15	3.64
pK_2[c]	10.78	11.13	10.54	10.29	11.61	11.52
pK_1[d]	3.79	3.04	3.29	4.25	3.05	3.52
pK_2[d]	10.86	11.12	10.52	10.35	11.64	11.66

[a] Uncertainties (SD) are shown in parentheses for the TSCs studied in the present work. [b] Taken from ref. 14 [c] Determined by pH-potentiometry. [d] Determined by UV-vis spectrophotometry.

UV-vis spectrophotometric titrations of FTSC, FaTSC and AcTSC revealed similar characteristic spectral changes with those for Triapine, PTSC and APTSC,[14] namely two intense absorption bands were found in the 260–450 nm wavelength range assigned to $n\rightarrow\pi^*$ transitions of the pyridine ring and the thiosemicarbazide moiety, which show alteration depending on the protonation states of the ligands. Starting at low pH (H_2L^+) both deprotonation steps resulted in changes in the absorption bands due to the extended conjugated electronic systems in the ligands. The first proton dissociation was accompanied by a blue shift, while during the second step a red shift was observed. Protonation constants and the spectra of the individual ligand species (H_2L^+; HL; L^-) (Table 2) were calculated on the basis of deconvolution of UV-vis spectra recorded at different pH values. Concentration distribution curves of AcTSC calculated with the help of these protonation constants, together with the absorbance at one of the λ_{max} values as a function of pH are shown in Fig. S1 in ESI.† Representative deconvoluted spectra of FaTSC and AcTSC are shown in Fig. 1. Spectra of individual FTSC species were similar to those reported in literature for pure aqueous solution.[16] It is noteworthy that the molar absorptivities (ε) of the FaTSC species are significantly lower compared with those of the other TSCs, especially H_2L^+ shows a quite weak absorption band at λ_{max} = 364 nm (see Table 2 and Fig. 1B). This can possibly be explained by a break in the conjugated electronic system of the molecule *via* migration of the

 This journal is © The Royal Society of Chemistry 2011

Table 2 λ_{max} and ε (mol^{-1} dm^3 cm^{-1}) values for $[H_2L]^+$, [HL] and $[L]^-$ ligand species determined by UV-vis spectrophotometric titrations (t = 25.0 °C, I = 0.10 mol dm^{-3} (KCl) in 30% (w/w) DMSO/H_2O) (Data for Triapine, PTSC, APTSC can be found in ref. 14)

	$[H_2L]^+$	[HL]	$[L]^-$
FTSC	354 nm (23.0×10^3) 268 nm (8.8×10^3)	316 nm (26.6×10^3)	353 nm (19.6×10^3)
FaTSC	364 nm (1.22×10^3)	316 nm (14.4×10^3)	340 nm (11.1×10^3)
AcTSC	348 nm (16.3×10^3) 268 nm (10.4×10^3)	308 nm (19.7×10^3)	344 nm (14.2×10^3)

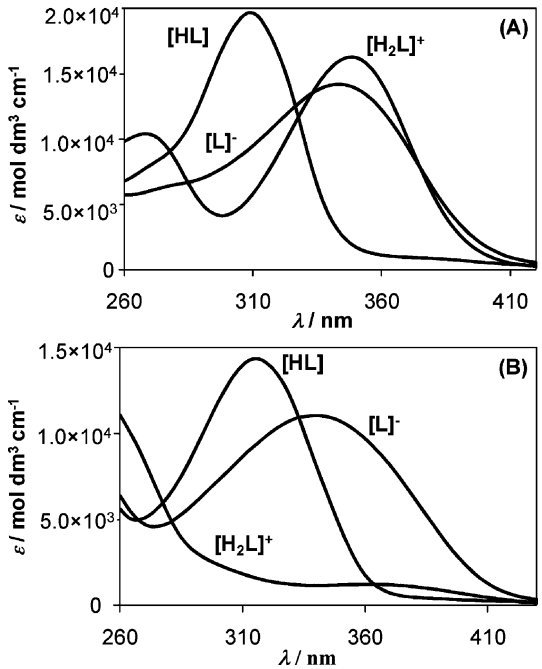

Fig. 1 Calculated UV-vis absorption spectra of the individual species of AcTSC (A) and FaTSC (B) {t = 25.0 °C, I = 0.10 mol dm^{-3} (KCl) in 30% (w/w) DMSO/H_2O}.

lone electron pair of the amino N at position R_2 to the adjacent C–N bond.

In comparison to the simplest α-*N*-heterocyclic thiosemicarbazone FTSC the amino and methyl substituents at the various positions have distinct influences on the proton dissociation constants. The addition of the electron-donating amino group at R_1 of the pyridine ring resulted in a significant increase in pK_1 and a small decrease in pK_2 (see data for Triapine *vs.* FTSC, or APTSC *vs.* PTSC in Table 1). The amino group at position R_2 has no effect on pK_1, whereas it increases pK_2 slightly (FaTSC *vs.* FTSC), and the methyl substituent at this position can increase both pK values (AcTSC *vs.* FTSC). Somewhat higher pK_1 and lower pK_2 were obtained in the case of the methyl groups on the terminal nitrogen (PTSC *vs.* FTSC, or APTSC *vs.* Triapine).

^{1}H NMR spectroscopic titrations were performed in order to follow the proton dissociation processes of Triapine and PTSC. In addition the different possible isomeric structures of the ligands can be investigated by this method (Scheme 2). Results show that Triapine exists exclusively in one isomeric form in 30% (w/w) DMSO/water in a wide pH range (~2–11) as H_2L^+ or HL. However, a new set of peaks of the C*H* protons of the pyridine ring appeared above pH 11, most probably due to isomerism of

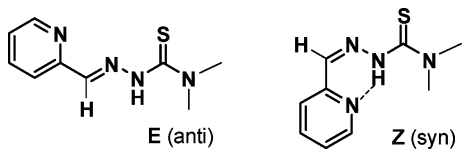

Scheme 2 Proposed structures for the isomers of HL species of PTSC.

the L^- species of Triapine (some representative ^{1}H NMR spectra of Triapine at different pH values are shown in Fig. S2 in ESI†). The amount of the new isomer reaches *ca.* 60% when the ligand becomes completely deprotonated, which was estimated from the integrated signals of the C*H*(pyr)(6) protons (see Fig. S2 in ESI†). Decomposition of the Triapine ligand can be excluded at this highly basic pH because back titration of the sample again showed only one set of signals at the lower pH values.

^{1}H NMR spectra of the terminally dimethylated PTSC revealed a different isomeric pattern compared with Triapine. Spectra of the individual species of PTSC, obtained at pH values where they are predominant, are illustrated in Fig. 2A. The spectrum of H_2L^+ consists of five peaks of the C*H*(pyr) and C*H*(=N) protons and one belonging to the methyl protons, all of them with a quite broad shape. Following the first deprotonation a doubled set of all the peaks appears in the spectrum of HL species most probably due to its isomerism. It was reported by Pessoa *et al.*, that when the equilibrium is reached between the isomers of PTSC species the ratio of the E(*anti*)/Z(*syn*) isomers (shown in Scheme 2) is 60/40

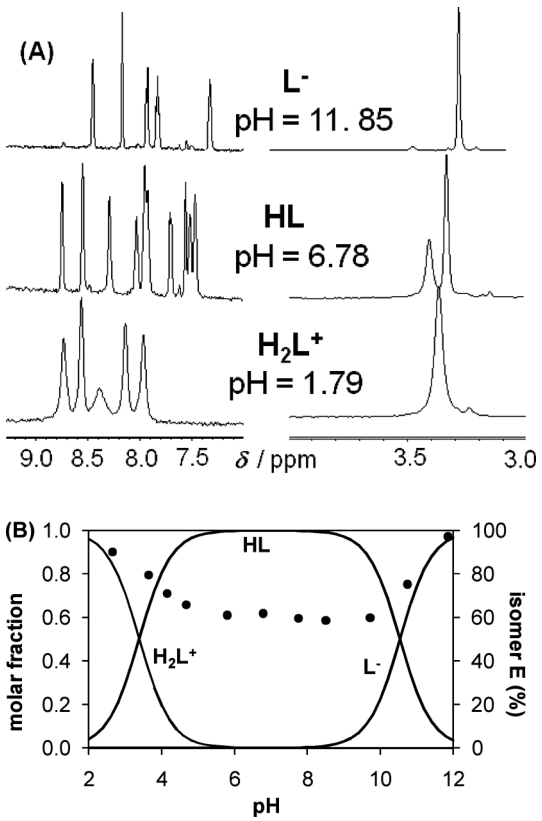

Fig. 2 Some representative ^{1}H NMR spectra of PTSC recorded at different pH values (A) and concentration distribution curves for PTSC with the % of the E(*anti*) isomer estimated on the basis of the integrated areas the of the signals of the N(C**H**$_3$)$_2$ protons (●) plotted against pH (B) {c_{ligand} = 1.0×10^{-3} mol dm^{-3} in 30% (w/w) d_6-DMSO/D_2O}.

Table 3 Fluorescence properties of the TSC ligands and of the Ga^{III}–TSC systems (c_{ligand} = 1 × 10^{-5} mol dm^{-3}; M:L = 1 : 2 in the case of Ga^{III} containing samples; t = 25.0 °C, I = 0.10 mol dm^{-3} (KCl) in 30% (w/w) DMSO/H_2O)

		λ_{EX}[a]	λ_{EM}[a] (Intensity[b])
Triapine	Ligand; pH 4.20[c]	360 nm	458 nm (770)
	Ga^{III}–TSC; pH 4.20[c]	430 nm	495 nm (870)
FTSC	Ligand; pH 5.00	320 nm	390 nm (144)
	Ga^{III}–TSC; pH 5.00	320 nm[d]	390 nm (151)[d]
PTSC	Ligand; pH 3.70[c]	328 nm	415 nm (490)
	Ga^{III}–TSC; pH 3.7[c]	395 nm	470 nm (246)
APTSC	Ligand; pH = 5.00	360 nm	428 nm (255)
	Ga^{III}–TSC; pH 5.00	440 nm	510 nm (>4000)
FaTSC	Ligand; pH 5.00	n.m[e]	n.m.[e]
	Ga^{III}–TSC; pH 5.00	n.m[e]	n.m[e]
AcTSC	Ligand; pH 5.00	n.m[e]	n.m.[e]
	Ga^{III}–TSC; pH 5.00	375 nm	470 nm (430)

[a] Maximum values. [b] PTM = 700 V; slits: 5–5 nm. [c] For more data at various pH values see Fig. 11 and S8 in ESI.† [d] It cannot be distinguished from the peak of ligand; at pH 3.6 ligand: λ_{EX} = 315 nm, λ_{EM} = 390 nm (I = 81), Ga^{III}–TSC: λ_{EX} = 315 nm, λ_{EM} = 390 nm (I = 120). [e] n.m. = Non measurable in the range of λ_{EX} = 300–600 nm.

in D_2O (pH not known) and 78/22 in d_6-DMSO as these solvents favor formation of hydrogen bonds between solvent molecules and the N*H*(C═S) resulting in the stabilization of the E isomer.[17] We also calculated the ratio of the two isomers from the integrated signals of the CH_3 protons at different pH values, which are displayed together with the speciation distribution diagram for PTSC in Fig. 2B. Our results confirm the *ca.* 60/40 isomer ratio of the E(*anti*)/Z(*syn*) forms in the pH range where the HL species is predominant (pH *ca.* 5–9). At higher pH values again only one isomer is present according to L^-.

Additionally, the TSCs were studied by spectrofluorimetric titrations. 3D fluorescence spectra of the ligands were recorded in order to obtain the excitation and emission wavelength maxima, which are summarized in Table 3. The 3D spectrum of PTSC is shown in Fig. 3A. An excitation maximum at 360 nm was found for Triapine and APTSC (R_1═NH_2) and at lower wavelengths for FTSC and PTSC (~325 nm), while no emission can be measured in the range of λ_{EX} = 300–600 nm in the case of ligands with R_2≠H (FaTSC and AcTSC). Fluorescence emission spectra were measured in dependence of pH for Triapine (see Fig. S3 in ESI†) and for PTSC (see Fig. 4A). They revealed that the emission intensity is strongly sensitive to the pH, and is changed parallel to both deprotonation steps. For comparison the fluorescence spectra of PTSC were also recorded without DMSO in aqueous

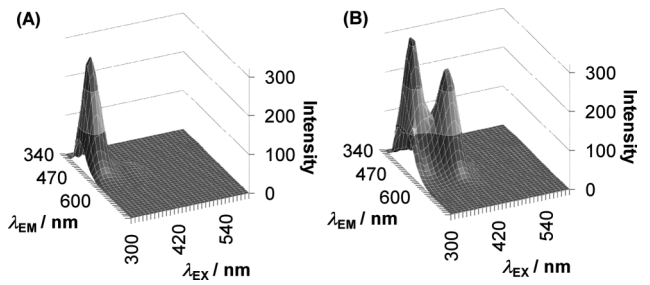

Fig. 3 3D fluorescence spectra of PTSC (A) and Ga^{III}–PTSC (B) systems {c_{ligand} = 5.2 × 10^{-6} mol dm^{-3}; Ga^{III}: PTSC = 1 : 1; pH = 4.20; λ_{EX} = 300–600 nm; t = 25.0 °C, I = 0.10 mol dm^{-3} (KCl)}.

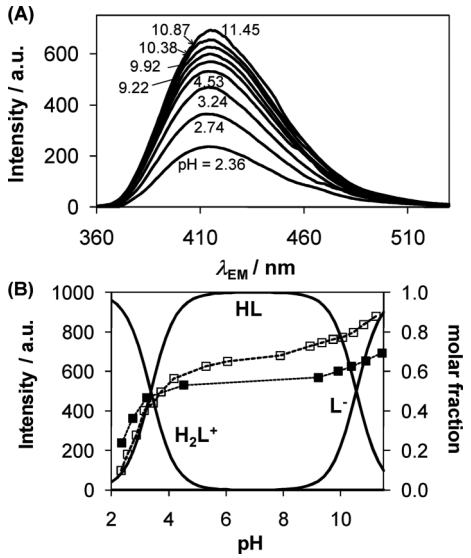

Fig. 4 Fluorescence emission spectra of PTSC recorded at different pH values in 30% (w/w) DMSO/H_2O (A) and concentration distribution curves for PTSC with the intensity of emission recorded at 415 nm in 30% (w/w) DMSO/H_2O (■) and in H_2O (□) (B) {λ_{EX} = 328 nm; c_{ligand} = 1.0 × 10^{-5} mol dm^{-3}; t = 25.0 °C, I = 0.10 mol dm^{-3} (KCl)}.

solution and the intensities are represented in Fig. 4B. The same excitation and emission maximum wavelength values were obtained for PTSC both in aqueous solution and in 30% (w/w) DMSO/H_2O. However, the H_2L^+ species showed a slightly lower, and HL and L^- a somewhat higher intensity in water. Intensity changes depending on the pH also suggest a somewhat higher pK_1 in the aqueous milieu. This corresponds well to the expectation that the pK values of cationic acids ($N_{pyr}H^+$) is decreased in the presence of DMSO as the dielectric permittivity of the solvent is decreased according to the Izmailov theory.[18] In agreement Legget *et al.* also obtained a somewhat higher pK_1 value (3.67) of FTSC in aqueous solution[16] compared to our pK_1 (3.13) measured in 30% (w/w) DMSO/H_2O. The pK_2 values of the TSCs are similar in both solvents.

Iron(II) and iron(III) complexes of the thiosemicarbazones

The complex formation processes of TSCs with Fe^{II} and Fe^{III} were studied by pH-potentiometry and UV-vis spectrophotometry in a 30% (w/w) DMSO/H_2O solvent mixture. The stoichiometries of the metal complexes and the cumulative stability constants furnishing the best fits to the experimental data are listed in Table 4. Since the coordination of the TSCs to Fe^{III} starts at pH < 2, the overall formation constants of the mono-ligand complexes formed at low pH were determined by spectrophotometry on individual samples following the changes of the metal-to-ligand charge transfer (CT) bands in the visible region (see Fig. 5A for APTSC). By fitting the spectra recorded between pH 1.0 and 2.0, the stability constants for $[Fe^{III}L]^{2+}$ complexes could be calculated. After keeping them constant the logβ values of $[Fe^{III}L_2]^+$ species were determined by spectrophotometry *via* the use of the CT bands between pH 2–10 (see Fig. 5B for APTSC; Fig. S4 in ESI† for FaTSC together with the calculated spectra of the individual iron complexes and the fitting between the measured and calculated absorbance values) and by pH-potentiometry. The

 This journal is © The Royal Society of Chemistry 2011

Table 4 Overall and derived stability constants ($\log\beta[M_pL_qH_r]$) for the Fe^{II}, Fe^{III} and Ga^{III} TSC complexes ($t = 25.0$ °C, $I = 0.10$ mol dm^{-3} (KCl) in 30% (w/w) DMSO/H_2O)[a]

	Triapine	FTSC	PTSC	APTSC	FaTSC	AcTSC
$\log\beta([Fe^{II}LH]^{2+})$[b]	15.91[c]	—	—	—	15.96(3)	—
$\log\beta([Fe^{II}L]^{+})$[b]	12.29[c]	12.48(3)	13.27[c]	14.37[c]	11.23(7)	14.37(3)
$\log\beta([Fe^{II}LH_{-1}])$[b]	—	—	—	8.92[c]	—	—
$\log\beta([Fe^{II}L_2H]^{+})$[b]	27.70[c]	26.2(1)	27.54[c]	29.09[c]	27.41(5)	28.35(9)
$\log\beta([Fe^{II}L_2])$[b]	22.55[c]	22.31(5)	23.37[c]	24.16[c]	21.59(8)	23.75(5)
$\log\beta([Fe^{II}L_2H_{-1}]^{-})$[b]	10.83[c]	—	—	—	10.44(9)	12.97(7)
Fitting parameter (mL)[b]	—	3.95×10^{-3}	—	—	4.88×10^{-3}	4.53×10^{-3}
No. of points[b]	—	145	—	—	216	97
$\log\beta([Fe^{II}L_2]) - 2 \times \log\beta(H_2L^{+})$	–6.85	–6.21	–4.47	–5.04	–7.93	–6.57
$\log\beta([Fe^{III}L]^{2+})$[d]	14.03(3)	14.48(2)	17.5(2)	15.48(2)	16.77(2)	16.69(3)
$\log\beta([Fe^{III}L_2]^{+})$[d]	26.25(5)	25.44(4)	30.89(7)	28.59(5)	30.51(4)	29.70(7)
No. of spectra[d]	25	24	15	47	37	27
$\log\beta([Fe^{III}L_2]^{+})$[b]	26.60(8)	25.36(5)	30.45(8)	28.87(7)	30.43(9)	30.44(9)
Fitting parameter (mL)[b]	5.56×10^{-3}	5.85×10^{-3}	9.81×10^{-3}	2.62×10^{-3}	8.53×10^{-3}	7.11×10^{-3}
No. of points[b]	98	123	137	118	180	108
$\log\beta([Fe^{III}L_2]^{+}) - 2 \times \log\beta(H_2L^{+})$	–2.80	–3.16	2.61	–0.33	0.91	0.12
pM[e]	15.7	14.3	20.4	18.9	17.9	17.3
$\log\beta([Ga^{III}LH]^{3+})$[b]	—	—	17.24(6)	16.80(8)	17.94(4)	18.50(5)
$\log\beta([Ga^{III}L]^{2+})$[b]	—	—	14.45(6)	—	—	—
$\log\beta([Ga^{III}L_2]^{+})$[b]	22.90(8)	22.2(1)	26.98(6)	26.39(9)	28.60(3)	28.03(4)
Fitting parameter (mL)[b]	6.82×10^{-3}	9.99×10^{-3}	3.78×10^{-3}	6.06×10^{-3}	7.84×10^{-3}	9.09×10^{-3}
No. of points[b]	124	150	210	169	120	121
$\log\beta([Ga^{III}L_2]^{+}) - 2 \times \log\beta(H_2L^{+})$	–6.50	–6.32	–0.86	–2.81	–0.92	–2.29

[a] Uncertainties (SD) are shown in parentheses for the complexes determined in the present work. [b] Determined by pH-potentiometry; $\beta(M_pL_qH_r) = [M_pL_qH_r]/[M]^p[L]^q[H]^r$; $pM + qL + rH \rightleftharpoons M_pL_qH_r$ *for the detailed equilibria see SI*. [c] Taken from ref. 14 [d] Determined by UV-vis spectrophotometric measurements. [e] pM = –log[Fe^{III}] at pH 7.40; $c_L/c_M = 10$; $c_M = 1$ μM; pM = 26.5 for desferrioxamine B; 19.3 for deferiprone; 20.3 for human serum transferrin; 24.3 for DOTA taken from ref. 20–22.

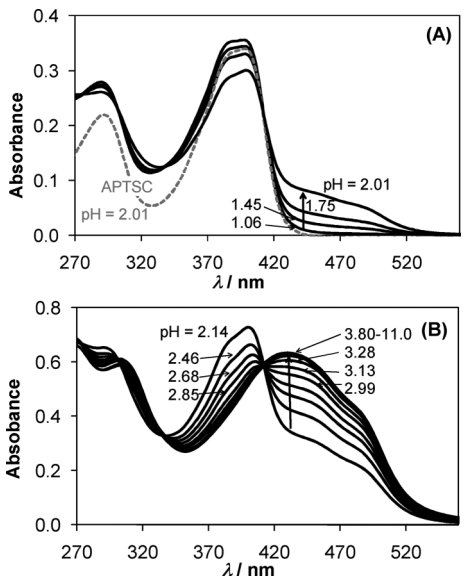

Fig. 5 UV-vis absorbance spectra of the Fe^{III}–APTSC system recorded at different pH values: pH < 2; $c_{ligand} = 2.0 \times 10^{-5}$ mol dm^{-3}; M:L = 1 : 1 (black solid lines) and 0 : 1 (grey dashed line) (A) and pH >2; $c_{ligand} = 5.0 \times 10^{-5}$ mol dm^{-3}; M:L = 1 : 1; (B) ($t = 25.0$ °C, $I = 0.10$ mol dm^{-3} (KCl) in 30% (w/w) DMSO/H_2O).

resulting constants obtained by the two methods are in good agreement. Stability constants of the Fe^{II}-TSC complexes were determined by pH-potentiometry (see Table 4) and data for Triapine, PTSC and APTSC were already published.[14] Besides $[Fe^{II}L]^{+}$ and $[Fe^{II}L_2]$, the formation of protonated $[Fe^{II}LH]^{2+}$, $[Fe^{II}L_2H]^{+}$, deprotonated $[Fe^{II}LH_{-1}]$ and $[Fe^{II}L_2H_{-1}]^{-}$ complexes could be also observed.

In the $[ML]^{+/2+}$ and $[ML_2]^{0/+}$ complexes of Fe^{II} and Fe^{III} the ligands most probably coordinate to the metal ions *via* the (N(pyr),N^1,S^-) donor set, as illustrated in Scheme 3. This mode of coordination was confirmed by X-ray diffraction for the Fe^{III} species.[8] In the protonated mono and *bis* ligand Fe^{II} complexes, the protons can presumably be attributed to the noncoordinating hydrazinic N^2 atom and again a (N(pyr),N^1,S) coordination mode can be suggested (see Scheme 3). The base consumption exceeding the number of dissociable protons in the ligands indicates that the species $[Fe^{II}LH_{-1}]$ and $[Fe^{II}L_2H_{-1}]^{-}$ formed at basic pH should be regarded as mixed hydroxido complexes $[Fe^{II}L(OH)]$ and $[Fe^{II}L_2(OH)]^{-}$, in which either the coordinated water molecules are deprotonated or a coordinated donor group is displaced by a OH^{-}.

Complex formation of Fe^{II} with the TSC ligands was additionally investigated by UV-vis spectrophotometric measurements under strictly anaerobic conditions. Spectra recorded at different pH values show that the (N(pyr),N,S^-) donor set and especially the coordination of the aromatic nitrogen atom in the complexes $[Fe^{II}L_2]$ resulted in broad CT bands with high molar absorptivity in the visible region in all systems studied. The formation of mono complexes resulted in a shoulder in the interval 450–500 nm, whereas formation of the *bis*-ligand species was accompanied by the development of an absorption band with maximum at *ca.* 610–620 nm as it was illustrated for Triapine in our previous work (see Fig. 5 in Ref. 14)

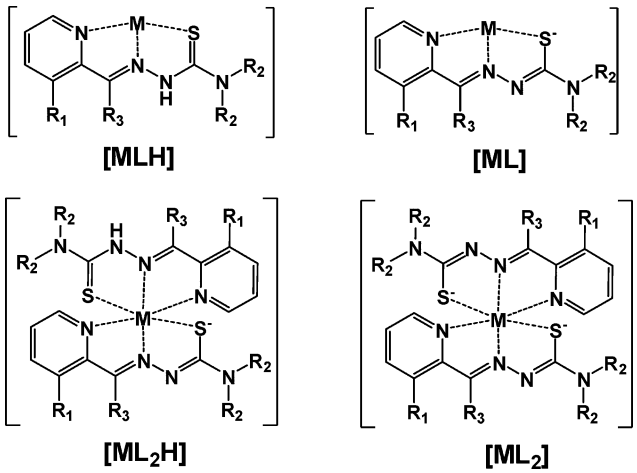

Scheme 3 Proposed structures of [MLH], [ML], [ML_2H] and [ML_2] complexes of Fe^{II}, Fe^{III} and Ga^{III}. (Charges of the complexes are omitted for simplicity.)

Based on the constants quoted in Table 4 it can be concluded that Fe^{II} forms complexes with considerably high stability; however compared with the Fe^{III} species they possess several orders of magnitude lower constants. The difference in the stability constants between the corresponding Fe^{II} and Fe^{III} complexes was found to be higher than that reported by Borger *et al.* for FTSC and ACTSC in aqueous solution.[19] It is important to note that both metal ions form the predominant [ML_2] species in a wide pH-range (especially in the case of Fe^{III}) as it is illustrated by the concentration distribution curves of AcTSC shown in Fig. 6. It should be also stressed that $[Fe^{III}L_2]^+$ is able to retain its original integrity almost completely with decreasing total concentration down to the micromolar range at neutral pH due to its prominent stability, while enhanced formation of the mono-ligand species is found in the highly diluted solution of $[Fe^{II}L_2]$ (see Fig. 10 in ref. 14).

As the coordination mode of the complexes [ML_2] formed with iron ions in solution is assumed to be similar (N(pyr),N^{-},S^{-}), the affinity of different TSC ligands towards the Fe^{II} and Fe^{III} can be compared by a correlation diagram as $\log\beta([Fe^{II}L_2])$ values are plotted against those of $[Fe^{III}L_2]^+$, which is represented in Fig. 7A. The diagram shows that a linear free energy relationship (LFER) is valid in tendency: the higher the $\log\beta([Fe^{III}L_2]^+)$ the higher the $\log\beta$ ($[Fe^{II}L_2]$), however the value of FaTSC falls well off the correlation, *i.e.* with stability constants of Fe^{II} considerably lower than expected.

Moreover, the stability constants of the [ML_2] species were corrected by the ligand basicities according to the following competition reaction:

$$M^{2+} + 2\ H_2L^+ \rightleftharpoons [ML_2] + 4\ H^+ \quad (1)$$

$$\log K = \log\beta([ML_2]) - 2\log\beta(H_2L^+) \quad (2)$$

The log K values as derived constants (see Table 4, Fig. 7B) can provide information about the chelate stability in the [ML_2] complexes. A higher log K implies more favoured metal complex formation as compared with the proton complex. Data show that PTSC is the most effective binder for both Fe^{II} and Fe^{III}. The chelate stability order for Fe^{III} is the following: FTSC ~ Triapine < APTSC ~ AcTSC < FaTSC < PTSC, while a similar trend can be also observed for Fe^{II} with the exception of FaTSC as its stability is the lowest.

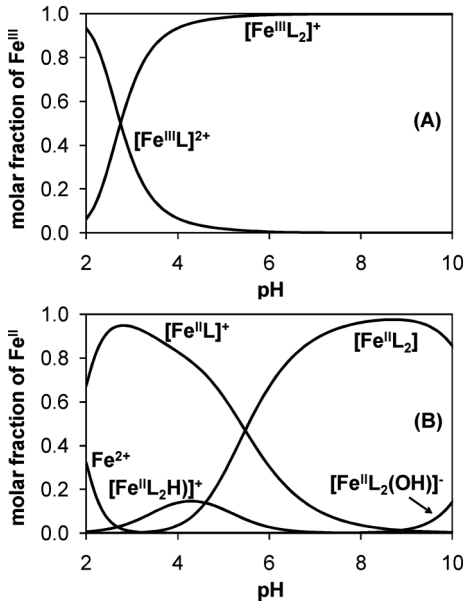

Fig. 6 Concentration distribution curves of iron complexes formed in the Fe^{III}–AcTSC (A) and Fe^{II}-AcTSC (B) systems at metal-ion-to-ligand ratio 1 : 2 calculated on the basis of the pH-potentiometric results, $c_{ligand} = 2.0 \times 10^{-3}$ mol dm^{-3}.

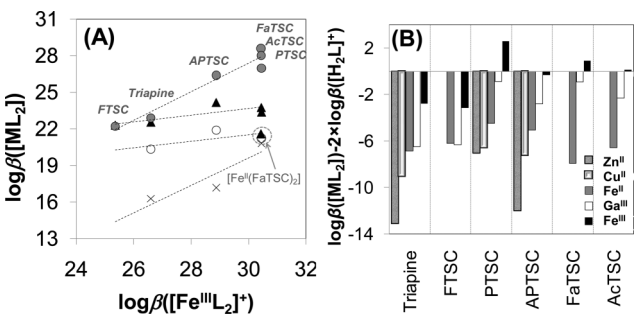

Fig. 7 Correlation (LFER) diagram for the *bis*-ligand complexes between $\log\beta[Fe^{III}L_2]^+$ and $\log\beta[ML_2]$ values of Ga^{III} (●); Fe^{II} (▲); Cu^{II} (○); Zn^{II} (×) (A); Stability constants of the *bis*-ligand complexes corrected with the ligand basicities ($\log K = \log\beta([ML_2]) - 2 \times \log\beta([H_2L]^+)$) (B) [See data in Table 4 for Fe^{III}, Ga^{III}, Fe^{II} and for Cu^{II} and Zn^{II} species data are taken from ref. 14].

In order to consider the Fe^{III} binding ability of the TSC ligands studied pM values were calculated at physiological pH (see Table 4) and are compared with some well-known iron-chelators such as desferrioxamine B,[20] Deferiprone,[21] human serum transferrin[20] and the macrocyclic DOTA.[22] It can be seen that the TSCs investigated are found to be efficient Fe^{III} binders, especially PTSC.

It is noteworthy that following the formation of the predominant *bis* Fe^{II}–TSC complexes the hydrolysis of the Fe^{II} species could be observed in the highly basic pH range. However, surprisingly the development of the characteristic CT bands of the Fe^{II} complexes in the 550–650 nm wavelength range was also detected in the Fe^{III}–TSC systems, with the exception of FaTSC, at pH > ~10 (depending on the ligand, the metal-to-ligand ratio, and ligand concentration) under strictly anaerobic conditions as seen in Fig. 8. When oxygen gas was bubbled through the samples the

 This journal is © The Royal Society of Chemistry 2011

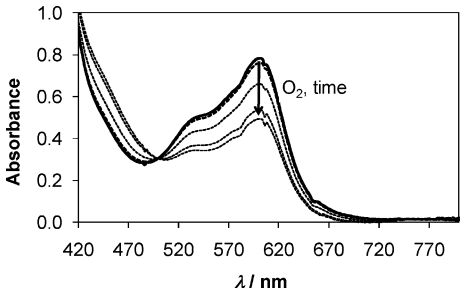

Fig. 8 UV-vis absorption spectrum of Fe^{III}–FTSC system recorded at pH = 11.50 under strictly aerobic conditions after 15 min incubation (black solid line) and after O_2 bubbling for *ca.* 1, 2, 3 h (grey dashed lines) {c_{ligand} = 1.0×10^{-3} mol dm^{-3}; metal-ion-to-ligand ratio 1 : 1.25; t = 25.0 °C, I = 0.10 mol dm^{-3} (KCl) in 30% (w/w) DMSO/H_2O}.

absorbance was slowly decreased due to the oxidation of Fe^{II}. Most probably the TSCs are able to reduce the bound Fe^{III}, while they are oxidized to the corresponding disulfides as it was shown for FTSC previously.[23]

In order to gain a better insight into the redox properties of the iron complexes cyclic voltammograms were measured for all the Fe^{III}-TSC systems studied at different pH values in 30% (w/w) DMSO/H_2O and a few illustrative voltammograms are shown in Fig. 9. Formal redox potential values of $[Fe^{III}L_2]^+$ complexes are collected in Table 5. It is noteworthy that similar values were also obtained in [*n*-Bu_4N][BF_4]/DMSO medium in our previous work.[8] The peak-to-peak potential separations and the peak current ratios indicate a reversible one electron transfer processes in pH range 5.0–9.2. Fe^{III} forms almost exclusively *bis*-ligand complexes in this pH range (see Table 4), which results in full reversibility and the molar fraction of the Fe^{II} reveals that *bis* species are also predominant at pH 7.5 and 9.2. Most probably the reduction/oxidation processes do not disturb considerably the coordination mode and geometry. By decreasing the pH below 3 the processes become more and more irreversible.

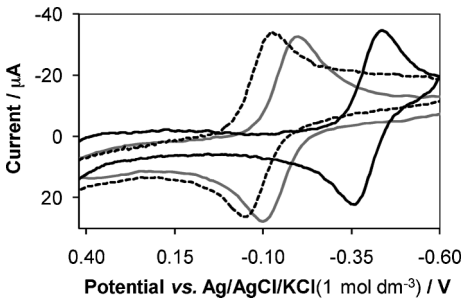

Fig. 9 Cyclic voltammograms of $[Fe^{III}L_2]^+$ complexes *vs.* Ag/AgCl/KCl (1.0 mol dm^{-3}) {t = 25.0 °C, I = 0.10 mol dm^{-3} (KCl) in 30% (w/w) DMSO/H_2O mixture at pH = 7.50. Metal-to-ligand ratio 1 : 2, c_{ligand} = 1.0×10^{-3} mol dm^{-3}. 0.01 V s^{-1} scan rate and Pt working electrode were applied}. (Black solid line: FaTSC; grey line: Triapine; black dashed line: PTSC).

The redox potential for the Fe^{III}/Fe^{II} couple is largely controlled by the donor ligands that are present in the first coordination shell. However, the same coordination modes and geometries are assumed for all the $[Fe^{III}L_2]^+$ TSC complexes, the influence of the substituents at the various positions of the TSC frame structure on their redox properties is clearly seen. As expected the NH_2 group

Table 5 Electrochemical data for $[Fe^{III}L_2]^+$ (HL = TSC)

	pH	$E'_{1/2}$ (V)[a]	ΔE (mV)[b]	i_a/i_c[c]	$x(Fe^{III})$[d]	$x(Fe^{II})$[d]
Triapine	5.00	**+0.07**	70	1.00	0.99	0.37
	7.50	**+0.07**	70	0.99	0.99	0.96
	9.20	**+0.07**	65	1.00	0.99	0.99
FTSC	5.01	**+0.17**	66	1.00	0.89	0.60
	7.50	**+0.16**	67	1.00	0.97	0.99
	9.21	**+0.16**	66	0.96	0.97	0.98
PTSC	5.02	**+0.15**	80	0.95	1.00	0.75
	7.50	**+0.14**	76	0.94	1.00	0.99
	9.22	**+0.13**	64	1.00	1.00	1.00
APTSC	5.00	**+0.05**	79	0.93	1.00	0.46
	7.50	**+0.05**	71	0.96	1.00	0.98
	9.21	**+0.04**	75	0.94	1.00	0.90
FaTSC	5.10	**–0.17**	66	0.83	0.99	0.11
	7.50	**–0.17**	66	0.69	1.00	0.93
	9.21	**–0.18**	71	0.85	1.00	0.99
AcTSC	5.01	**+0.05**	72	0.95	0.98	0.27
	7.50	**+0.04**	70	0.95	1.00	0.90
	9.22	**+0.04**	73	0.92	1.00	0.97

[a] Formal redox potential values of $[Fe^{III}L_2]^+$ complexes *vs.* NHE at t = 25.0 °C, I = 0.10 mol dm^{-3} (KCl) in 30% (w/w) DMSO/H_2O mixture at different pH; $c(Fe^{III}) = 1 \times 10^{-3}$ mol dm^{-3}; M:L = 1 : 2. [b] Peak potential separation ($\Delta E = E_a - E_c$) (a: anode; c: cathode). [c] Peak current ratio. [d] Molar fraction of Fe calculated at $c(Fe^{III}) = 1 \times 10^{-3}$ mol dm^{-3}; M:L = 1 : 2.

at position R_1 decreases the iron redox potentials, by ~100 mV (Triapine *vs.* FTSC, or APTSC *vs.* PTSC in Table 5) and at R_2 by ~300 mV (FaTSC *vs.* FTSC). Also the methyl substituent at the azomethine group shifts the reduction wave to lower potentials (~100 mV; AcTSC *vs.* FTSC), whereas the terminal dimethylation does not exert a measurable effect on the redox potentials (PTSC *vs.* FTSC, or APTSC *vs.* Triapine).

Thus among the Fe^{III}/Fe^{II} couples studied the FaTSC complexes possess the most negative potential (see Table 5), which indicates a preference for the higher oxidation state as it is reflected in the relatively low stability of the Fe^{II} complexes of FaTSC and the absence of reduction of Fe^{III} by the ligand at very high pH values (see above).

It should be stressed that all the formal potential values of the iron TSC complexes lie within a range accessible to intracellular oxidants and reductants such as NADPH, thiols, *etc.*[8,24] This fact and the reversibility of redox couples contribute to ROS generation under physiological conditions, responsible at least in part for their antiproliferative activity.[7,24]

Gallium(III) complexes of the thiosemicarbazones

Stability constants for the Ga^{III}–TSC complexes were calculated on the basis of the analysis of the titration curves obtained by pH-potentiometry in 30% (w/w) DMSO/H_2O and are collected in Table 4. Formation of relatively high stability mono-ligand ($[GaLH]^{3+}$ and $[GaL]^{2+}$) and *bis*-ligand ($[GaL_2]^+$) species was found. The complexation starts somewhat below pH 2 as proton displacement by the metal ion could be observed by changes of the ligand bands in the UV-vis spectra recorded at such low pH values (see Fig. S5 in ESI†). In these Ga^{III} complexes tridentate ($N(pyr),N^1,S^-$) binding of the TSC ligands studied is assumed in solution (see Scheme 3) taking into account the X-ray diffraction studies of the species $[GaL]^{2+}$ and $[GaL_2]^+$.[8]

It is worth noting that the stabilities of the complexes $[GaL_2]^+$ are lower than those of the corresponding Fe^{III} species by 2–3 orders of magnitude and they show an unambiguous linear correlation with $\log\beta([Fe^{III}L_2]^+)$ values as it is illustrated in Fig. 7A; consequently, the stability constants of *bis*-ligand gallium complexes corrected by the ligand basicities give a similar stability sequence of the TSCs as it was obtained in the case of Fe^{III} complexes (see Fig. 7B and Table 4 for the log *K* values). Comparing the stabilities of the *bis*-ligand complexes in the case of different metal ions (see Fig. 7B) the following general stability order was found: $Zn^{II} < Cu^{II} < Fe^{II} < Ga^{III} \ll Fe^{III}$, however, our results also revealed the different pH range for the formation of these complexes.

A species-distribution diagram for Ga^{III}–FaTSC system is shown in Fig. 10A. This diagram, calculated at millimolar concentrations, reveals first of all, that the $[GaL_2]^+$ complex predominates in the slightly acidic pH range, whilst the gallium species tends to hydrolyze already at neutral pH accompanied by the formation of the water soluble Ga^{III}-hydroxido species. The molar fraction of the *bis* complexes is significantly diminished with decreasing complex concentration at neutral pH due to hydrolysis (see Fig. 10B) in accord with the general expectations.

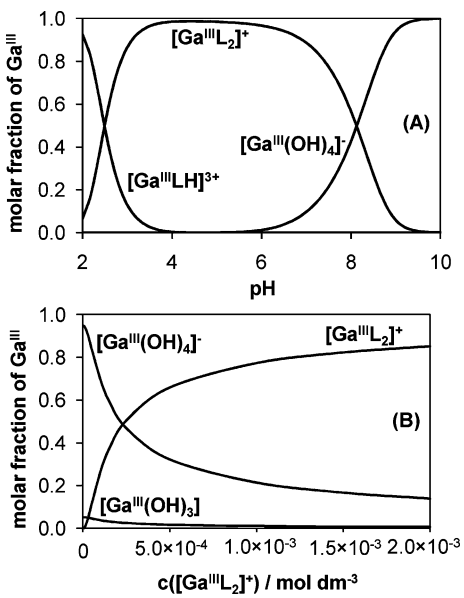

Fig. 10 Representative concentration distribution diagram for Ga^{III} complexes formed in the Ga^{III}–FaTSC system plotted against the pH at metal-ion-to-ligand ratio 1 : 2 calculated on the basis of the pH-potentiometric results, $c_{ligand} = 2.0 \times 10^{-3}$ mol dm^{-3} (A) and at various total concentrations of the $[Ga^{III}L_2]^+$ complex at pH 7.50 (B).

Electrospray ionization mass spectrometry (ESI-MS) for the Ga^{III}–PTSC system at acidic pH also indicates the exclusive formation of complex $[GaL_2]^+$ (for the experimental details and spectra see Fig. S6 in ESI†), however, the relative abundance of the metal-free ligand is increased significantly compared to that of the *bis* complex with increasing pH as a result of the hydrolysis. Since generally the quantitative reliability of ESI-MS results is not satisfactory, other methods such as spectrofluorimetry and ^{1}H NMR spectroscopy were used to get an insight into the speciation of the Ga^{III}-TSC complexes (in addition to pH-potentiometry).

Fluorimetric titrations of fluorescent ligands or their metal complexes may provide information about the pH range of complex formation processes. The measurements were performed at micromolar concentrations, which is advantageous in terms of the solubility problems. In addition, this is the concentration range of the biological activity of some of the Ga^{III} complexes too.[8] It was found that in the presence of Ga^{III} an extra peak appeared in the 3D fluorescence spectrum in addition to the ligand's peak with a higher excitation wavelength maximum as Fig. 3B and S7B in ESI† show for PTSC and Triapine, respectively. Maximum values of λ_{EX} and λ_{EM} obtained for the Ga^{III}–TSC systems at around the pH of the assumed maximal formation of the Ga^{III} complexes are collected in Table 3 (in the case of FaTSC neither the ligand nor its Ga^{III} complexes show fluorescence in the λ_{EX} range studied). Fluorescent behavior of Ga^{III}-FTSC and other Ga^{III}-2-acetylpyridine TSC complexes was already reported, however, the pH-dependence has not been studied.[25,26] Changes in the emission intensities were followed at the λ_{EX} maxima of the additional peak obtained in the presence of gallium as a function of the pH in the case of Ga^{III}–PTSC and Ga^{III}–Triapine systems (see Fig. 11 and S8 in ESI†).

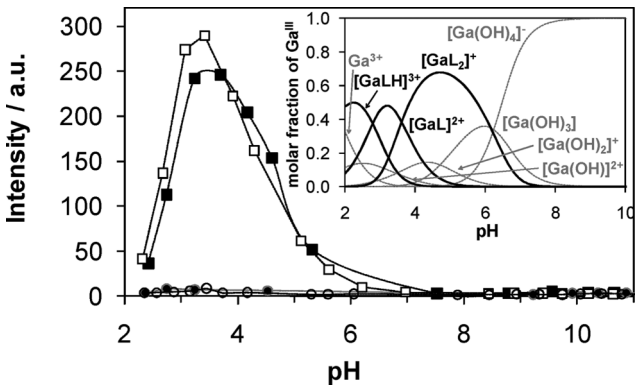

Fig. 11 Fluorescence emission intensity recorded at 470 nm for Ga^{III}–PTSC (1 : 2) system (■) and for the metal-free PTSC (●) at different pH values {λ_{EX} = 395 nm; $c_{ligand} = 1.0 \times 10^{-5}$ mol dm^{-3}; t = 25.0 °C, I = 0.10 mol dm^{-3} (KCl) in 30% (w/w) DMSO/H_2O}. In addition to the values recorded in pure aqueous solution for Ga^{III}–PTSC (1 : 2) system (□) and for the metal-free PTSC (○). *Inset shows the concentration distribution curves of gallium complexes formed in the Ga^{III}–PTSC system plotted against the pH under the corresponding conditions.*

For comparison the metal-free ligands were measured. The experimental runs reveal that the emission of the ligands in the absence of metal ion is negligible at the chosen λ_{EX}, while in the presence of Ga^{III} the fluorescence intensity shows a strong pH-dependence. Considering the calculated speciation diagram (see inset of Fig. 11) the recorded emission values suggest that the intensity is raised roughly in the pH range where Ga^{III}–TSC complexes are present, and that $[GaL]^{2+}$ has the most prominent contribution to the emission signal. Similar spectrofluorimetric titrations were performed in aqueous solutions without DMSO (see Fig. 11) and results are comparable to those obtained in the DMSO/H_2O solvent mixture.

^{1}H NMR spectra were recorded at different pH values merely for the highest stability Ga^{III}–PTSC complexes (see Fig. 12), which were compared with those of the metal-free PTSC (see Fig. 2A).

First of all a slow ligand-exchange process was found with respect to the NMR time scale as the chemical shifts of the protons of the metal-free and the metal-bound ligand could be

 This journal is © The Royal Society of Chemistry 2011

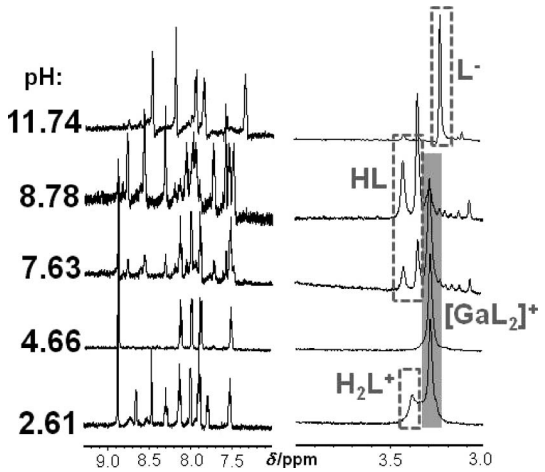

Fig. 12 ^{1}H NMR spectra of the Ga^{III}–PTSC system at selected pH values at metal-ion-to-ligand ratio 1 : 2 {$c_{ligand} = 1.0 \times 10^{-3}$ mol dm^{-3} in 30% (w/w) d_6-DMSO/D_2O}. (For additional spectra see Fig. S10†).

seen separately. At pH ~ 2.6, the relatively broad peaks of the ligand (H_2L^+) appear in addition to those of the gallium complexes formed (mainly $[GaL_2]^+$ see Fig. 12 and S9 in ESI†). The complex $[GaL_2]^+$ displays five well-resolved peaks of the C*H*(pyr) and C*H*(–N) protons and a single peak of the methyl protons between pH ~ 4–7 showing the predominant formation of this species and the lack of the metal-free ligand (see Fig. 12 and the ^{1}H NMR spectrum with the proton assignments in Fig. S11 in ESI†). The presence of the isomers of the HL form (see Fig. 12 and 2A) and the decreasing intensity of the signals belonging to the *bis*-ligand complex can be identified at pH > 7.5. At higher pH values the spectra become identical to those of the ligand alone at the same pH range (Fig. 2A).

All these findings are consistent with the speciation suggested by the pH-potentiometric results, *i.e.* TSCs are able to bind Ga^{III} strongly in the acidic pH range, but significant hydrolysis of Ga^{III} takes place at the physiological pH and it is more pronounced as the solution is more diluted. However, it is still a question how the dissociation processes are influenced by the cell or human blood serum components *in vivo*, especially in the case of the higher stability Ga^{III} complexes with terminally dimethylated TSC ligands like PTSC.

Relationship between stability and biological activity

In order to obtain a view of the most probable forms of the metal complexes administered for the activity measurements in the biological milieu, speciation diagrams can be calculated on the basis of the stability constants at relevant concentration conditions. This may be an important link between the solid phase and the biological studies, which can help the mechanistic explanations of the cytotoxicity. Our results suggest that Fe^{III} is mostly bound in the *bis*-ligand complexes in the diluted solutions at neutral pH, but the Ga^{III} complexes tend to hydrolyze.

The cytotoxicity studies[8] (see IC_{50} values in Table S1 in ESI†) showed that the dimethylation of the terminal NH_2 group can strongly enhance the activity of the ligands (*e.g.* FTSC *vs.* PTSC), however this effect is minor in the presence of an amino group at positions R_1 or R_2 (*e.g.* APTSC). The presence of an amino or methyl group at position R_2 decreases the ligands' cytotoxicity.[8] The same structure-activity relationship was obtained for the *bis*-ligand Ga^{III} complexes. The similar IC_{50} values of the metal-free ligands and their Ga^{III} complexes (taking into account the stoichiometry of the $[GaL_2]^+$ species) imply that the biological activity of the complex is largely governed by the ligand due to the extended hydrolysis of the complex. In contrast, the species $[Fe^{III}L_2]^+$ show reduced cytotoxicity in comparison to that of the corresponding metal-free ligands. This is probably at least in part due to a reduced ability of the positively charged complex to cross the cell membrane. Interestingly, the ratio of the IC_{50} values of metal-free ligand and its Fe^{III} complex varies between 2 and 56 (see Table S1 in ESI†). $[Fe^{III}(PTSC)_2]^+$, which is the highest stability complex, has an outstanding biological activity among the Fe^{III} species due to the absence of any NH_2 group in the complex, but no unambiguous relationship between the IC_{50} values of complexes $[Fe^{III}L_2]^+$ and the stability trend of the iron complexes was found. Considering the ratios of the IC_{50} values of the complexes and TSCs it can be concluded that the decrease of the activity by the coordination of Fe^{III} is less pronounced in the case of the lower stability complexes of Triapine and FTSC.

Conclusions

Stoichiometry and stability of the complexes of six α-N heterocyclic thiosemicarbazones with potential antitumor activity with Ga^{III}, Fe^{III}, Fe^{II} were studied in partially aqueous solution focusing on the most plausible species emerging at physiological pH. We can conclude based on the results that the introduction of an amino group at the position R_1 of the pyridine ring (Scheme 1) only slightly decreases the chelate stabilities. At the same time the NH_2 group attached at the carbon atom of the azomethine group (at position R_2) can increase markedly the stability of the complexes formed with the trivalent metal ions, while a considerable decrease in the stability was established with Fe^{II}, and this different behavior was explained by the quite low formal redox potential of the Fe^{III}/Fe^{II} couple in the case of FaTSC. The substitution of the hydrogen atom by a methyl group at the position R_2 results in an enhancement of the complex stability. However, dimethylation of the terminal nitrogen of the TSCs (R_3) has the strongest stability increasing effect and PTSC is proved to be the most effective metal ion binder among the TSCs studied. A similar stability trend was reported for the Cu^{II} and Zn^{II} complexes in our recent work.[14] The *bis*-ligand complexes $[ML_2]$ are usually applied to investigate the biological activities, and it was found that *bis*-ligand complexes of Fe^{III} and Fe^{II} predominate, whilst Ga^{III} complexes tend to hydrolyze at physiological pH in the diluted solutions.

We discovered that most of the TSC ligands studied and their Ga^{III} complexes are highly fluorescent, which makes monitoring of the extra- and intracellular distribution of the ligands or fluorimetric determination of Ga^{III} possible.

Concerning the intracellular formation of a metal complex these results further support the assumption that if TSCs form a metal complex inside cells only iron comes into question, due to its very high stability complexes with TSCs and the extremely low free copper and zinc levels in cells.

Our conclusions emphasize the importance of the knowledge of the actual chemical forms of the metal complexes in the aqueous solutions administered for the biological studies and that the cytotoxic activity is influenced by a large number of parameters

such as the structure, charge, redox properties, stability of the metal complexes *etc.* besides other important factors such as lipophilicity and ability to interact with exogenous bioligands *e.g.* human serum transferrin. Thus, characterization of the complexes in terms of these latter properties is underway in our laboratories.

Experimental

Chemicals

Triapine and all other thiosemicarbazones (FTSC, PTSC, APTSC, FaTSC and AcTSC) were prepared as described previously.[8] The purity and stability of the ligands was checked and the exact concentrations of the stock solutions prepared were determined by the Gran method.[27] The Fe^{II} stock solution was obtained from fine Fe powder dissolved in a known amount of HCl solution under a purified, strictly oxygen-free argon atmosphere, then filtered, stored and used under anaerobic conditions. KSCN (Sigma-Aldrich) solution was used to check the absence of Fe^{III} traces in the Fe^{II} solution. The concentration of the Fe^{II} stock solution was determined by permanganometric titrations under acidic conditions. Ga and $FeCl_3$ were dissolved in a known amount of HNO_3 and HCl, respectively, in order to get the Ga^{III} and Fe^{III} stock solutions. Their concentrations were determined by complexometry *via* the EDTA complexes. Accurate strong acid content of the metal stock solutions were determined by pH-potentiometric titration.

pH-potentiometric measurements

The pH-metric measurements for determination of the protonation constants of the ligands and the overall stability constants of the metal complexes were carried out at 25.0 ± 0.1 °C in DMSO:water 30 : 70 (w/w) as solvent and at an ionic strength of 0.10 mol dm^{-3} (KCl, Sigma-Aldrich) in order to keep the activity coefficients constant. The titrations were performed with carbonate-free KOH solution of known concentration (0.10 mol dm^{-3}). Both the base and the HCl used were Sigma-Aldrich products and their concentrations were determined by pH-potentiometric titrations. An Orion 710A pH-meter equipped with a Metrohm combined electrode (type 6.0234.100) and a Metrohm 665 Dosimat burette were used for the pH-metric measurements. The electrode system was calibrated to the pH = log[H^+] scale in the DMSO/water solvent mixture by means of a blank titrations (strong acid *vs.* strong base; HCl *vs.* KOH),[28] similarly to the method suggested by Irving *et al.*[29] in pure aqueous solutions. The average water ionization constant, pK_w, is 14.52 ± 0.05 with DMSO:water 30 : 70 (w/w) as solvent at 25 °C, which corresponds well to the literature data.[14,30] The reproducibility of the titration points included in the calculations was within 0.005 pH. The pH-metric titrations were performed in the pH range 2.0–12.0. The initial volume of the samples was 5.0 or 10.0 mL. The ligand concentration was in the range 1–2 × 10^{-3} mol dm^{-3} and metal ion to ligand ratios of 1 : 1–1 : 4 were used. The accepted fitting of the titration curves was always less than 0.01 mL. Samples were deoxygenated by bubbling purified argon through them for *ca.* 10 min prior to the measurements. In the case of Fe^{II} samples, argon overpressure was used when Fe^{II} was added to the samples in tightly closed vessels, which were prior completely deoxygenated by bubbling a stream of purified argon through them for *ca.* 20 min. Argon was also passed over the solutions during the titrations.

The protonation constants of the ligands were determined with the computer program SUPERQUAD;[31] PSEQUAD[32] was utilized to establish the stoichiometry of the complexes and to calculate the stability constants (log $\beta M_pL_qH_r$)) using the literature data for Fe^{III} and Ga^{III} hydroxido complexes.[33,34] β $M_pL_qH_r$ is defined for the general equilibrium $pM + qL + rH \rightleftharpoons M_pL_qH_r$ as $\beta(M_pL_qH_r) = [M_pL_qH_r]/[M]^p[L]^q[H]^r$ where M denotes the metal ion and L the deprotonated ligand. Using this calibration protocol, the protonation and stability constants involving [H^+] were obtained and are considered as K_{mixed} (or practical) constants[35] and are valid only under the given circumstances. The calculations were always made from the experimental titration data measured in the absence of any precipitate in the solution.

UV-vis spectrophotometric, spectrofluorimetric and ^{1}H NMR measurements

A Hewlett Packard 8452A diode array spectrophotometer was used to record the UV-vis spectra in the interval 260–820 nm. The path length was 1 cm. Protonation and stability constants and the individual spectra of the species were calculated by the computer program PSEQUAD.[32] The spectrophotometric titrations were performed on samples of the pure TSCs or with Fe^{III} or Fe^{II}; the concentration of ligand was 5 × 10^{-5} mol dm^{-3} and the metal-to-ligand ratios were 0 : 1, 1 : 1 and 1 : 2 over the pH range between 2 and 12 at an ionic strength of 0.10 mol dm^{-3} (KCl) in 30% (w/w) DMSO/H_2O at 25.0 ± 0.1 °C. For Fe^{II} samples, spectra were recorded under anaerobic conditions. Measurements for 2 × 10^{-5} mol dm^{-3} TSC and 2 × 10^{-5} mol dm^{-3} Fe^{III} (or Ga^{III}) containing systems were also carried out by preparing individual samples in which the 0.1 mol dm^{-3} KCl was partially or completely replaced by HCl and pH values, varying in the range *ca.* 1.0–1.8, were calculated from the HCl content. For the calculation of the stability constants of Fe^{III}–TSC complexes CT bands were used (Triapine: λ > 450 nm; FTSC: λ > 420 nm; PTSC: λ > 430 nm; APTSC: λ > 412 nm; FaTSC: λ > 420 nm; AcTSC: λ > 420 nm).

The pH-dependent fluorescence measurements were carried out on a Hitachi-4500 spectrofluorimeter with the excitation at 360/430 nm or 328/395 nm for Triapine and PTSC containing samples, respectively. The emission spectra were recorded using 10 nm/10 nm slit widths in 1 cm quartz cell in the pH range between 2 and 12 in 30% (w/w) DMSO/H_2O (or water) at 25.0 ± 0.1 °C. Samples contained 1 × 10^{-5} mol dm^{-3} TSCs alone or with 5 × 10^{-6} mol dm^{-3} Ga^{III} at 0.1 mol dm^{-3} (KCl) ionic strength. Three-dimensional spectra were recorded at 300–600 nm excitations and at 330–800 nm emission wavelengths for the Ga^{III} and 5–10 × 10^{-6} mol dm^{-3} TSC ligand containing sample at metal-to-ligand ratios 1 : 1 or 1 : 2 at the pH value where the formation of the *bis*-ligand complex supposed to be maximal on the basis of the pH-potentiometric results.

^{1}H NMR studies were carried out on a Bruker Ultrashield 500 Plus instrument. TSCs were dissolved in a 30% (w/w) d_6-DMSO/D_2O mixture in a concentration of 1–4 × 10^{-3} mol dm^{-3} and the Ga^{III}-to-ligand ratios were 0 : 1 and 1 : 2. The direct pH-meter readings (pH*) in the deuterated solvent mixture obtained by the pH-meter calibrated in the 30% (w/w) DMSO/H_2O

 This journal is © The Royal Society of Chemistry 2011

according to Irving *et al.*[28] were converted to pH by the following equation: pH = pH* + 0.4.

Cyclic voltammetry

Cyclic voltammograms of the Fe^{III} complexes in 30% (w/w) DMSO/water solution containing 1×10^{-3} mol dm^{-3} Fe^{III} and 2 mM TSC ligand were determined at 25.0 ± 0.1 C° at different pH values. Ionic strength was 0.10 mol dm^{-3} (KCl). Measurements were performed on a conventional three-electrode system under nitrogen atmosphere and a PC Controlled Electrochemical Measurement System (EF 451). Samples were purged for 15 min with Ar before recording the cyclic voltammograms. Platinum electrode was used as the working and auxiliary electrode and Ag/AgCl (in 1 mol dm^{-3} KCl) as reference electrode. Electrochemical potentials were converted into the normal hydrogen electrode (NHE) scale by adding 0.222 V. The electrochemical system was calibrated with an aqueous solution of $K_3[Fe(CN)_6]$ ($E_{1/2}$ = +0.386 V *vs.* NHE).[36] Redox potentials were obtained at 10 mV s^{-1} scan rate in the range of –0.75 to +0.50 V.

Abbreviations

AcTSC	2-**ac**etylpyridine **t**hio**s**emi**c**arbazone
APTSC	3-**a**mino**p**yridine-2-carboxaldehyde N^4,N^4-dimethyl-**t**hio**s**emi**c**arbazone
CT	charge transfer
δ	chemical shift
DMSO	dimethyl sulfoxide
ESI-MS	electrospray ionization mass spectrometry
ε	molar absorptivity
FaTSC	2-pyridine**form**a**m**ide **t**hio**s**emi**c**arbazone
FTSC	2-**f**ormylpyridine **t**hio**s**emi**c**arbazone
λ_{EM}	fluorescence emission wavelength
λ_{EX}	fluorescence excitation wavelength
PTSC	**p**yridine-2-carboxaldehyde N^4,N^4-dimethyl**t**hio**s**emi-**c**arbazone
ROS	reactive oxygen species
RR	ribonucleotide reductase
TSC	**t**hio**s**emi**c**arbazone
Triapine	3-aminopyridine-2-carboxaldehyde thiosemicarbazone

Acknowledgements

This work has been supported by the Hungarian Research Foundation OTKA K77833, the Hungarian-Austrian Action Foundation and "TÁMOP-4.2.1/B-09/1/KONV-2010-0005 - Creating the Center of Excellence at the University of Szeged" is supported by the European Union and co-financed by the European Regional Fund. É.A.E. gratefully acknowledges the financial support of Bolyai J. research fellowships and C.R.K the Austrian Science Fond (FWF, grant P22072). We thank Mrs. Katalin Tóth-Szűcs for performing the pH-potentiometric measurements.

References

1 D. X. West, S. B. Padhye and P. B. Sonawane, *Struct. Bonding (Berlin)*, 1991, **76**, 1.
2 C. M. Nutting, C. M. L. van Herpen, A. B. Miah, S. A. Bhide, J. P. Machiels, J. Buter, C. Kelly, D. de Raucourt and K. J. Harrington, *Ann. Oncol.*, 2009, **20**, 1275.
3 D. R. Richardson, P. C. Sharpe, D. B. Lovejoy, D. Senatatne, D. S. Kalinowski, M. Islam and P. V. Bernhardt, *J. Med. Chem.*, 2006, **49**, 6510.
4 Y. Yu, D. S. Kalinowski, Z. Kovacevic, A. R. Siafakas, P. J. Jansson, C. Stefani, D. B. Lovejoy, P. C. Sharpe, P. V. Bernhardt and D. R. Richardson, *J. Med. Chem.*, 2009, **52**, 5271.
5 M. Whitnall, J. Howard, P. Ponka and D. R. Richardson, *Proc. Natl. Acad. Sci. U. S. A.*, 2006, **103**, 14901.
6 N. Birch, X. Wang and H. S. Chong, *Expert Opin. Ther. Pat.*, 2006, **16**, 1533.
7 J. Shao, B. Zhou, A. J. Di Bilio, L. Zhu, T. Wang, C. Q. J. Shih and Y. Yen, *Mol. Cancer Ther.*, 2006, **5**, 586.
8 C. R. Kowol, R. Trondl, P. Heffeter, V. B. Arion, M. A. Jakupec, A. Roller, M. Galanski, W. Berger and B. K. Keppler, *J. Med. Chem.*, 2009, **52**, 5032.
9 C. R. Kowol, R. Berger, R. Eichinger, A. Roller, M. A. Jakupec, P. P. Schmidt, V. B. Arion and B. K. Keppler, *J. Med. Chem.*, 2007, **50**, 1254.
10 S. Adsule, V. Barve, D. Chen, F. Ahmed, Q. P. Dou, S. Padhye and F. H. Sarkar, *J. Med. Chem.*, 2006, **49**, 7242.
11 D. Kovala-Demertzi, A. Alexandratos, A. Papageorgiou, P. N. Yadav, P. Dalezis and M. A. Demertzis, *Polyhedron*, 2008, **27**, 2731.
12 I. C. Mendes, M. A. Soares, R. G. dos Santos, C. Pinheiro and H. Beraldo, *Eur. J. Med. Chem.*, 2009, **44**, 1870.
13 C. R. Kowol, E. Reisner, I. Chiorescu, V. B. Arion, M. Galanski, D. V. Deubel and B. K. Keppler, *Inorg. Chem.*, 2008, **47**, 11032.
14 E. A. Enyedy, N. V. Nagy, E. Zsigo, C. R. Kowol, V. B. Arion, B. K. Keppler and T. Kiss, *Eur. J. Inorg. Chem.*, 2010, **11**, 1717.
15 C. R. Kowol, R. Trondl, V. B. Arion, M. A. Jakupec, I. Lichtscheidl and B. K. Keppler, *Dalton Trans.*, 2010, **39**, 704.
16 D. J. Leggett and W. A. E. McBryde, *Talanta*, 1974, **21**, 1005.
17 M. M. B. Pessoa, G. F. S. Andrade, V. R. P. Monteiro and M. L. A. Temperini, *Polyhedron*, 2001, **20**, 3133.
18 N. A. Izmailov, *Electrochemistry of solutions*, 2nd ed., Khimia, Moscow, 1966.
19 R. U. Borges, E. Paniago and H. Beraldo, *J. Inorg. Biochem.*, 1997, **65**, 267.
20 R. J. Motekaitis and A. E. Martell, *Inorg. Chim. Acta*, 1991, **183**, 71.
21 M. A. Santos, M. Gil, S. Marques, L. Gano, G. Cantinho and S. Chaves, *J. Inorg. Biochem.*, 2002, **92**, 43.
22 *Critically Selected Stability Constants of Metal Complexes Database*, ed. A. E. Martell, R. M. Smith and R. J. Motekaitis, College Station TX, Version 4.0, 1997.
23 J. García-Tojal, B. Donnadieu, J. P. Costes, J. L. Serra, L. Lezama and T. Rojo, *Inorg. Chim. Acta*, 2002, **333**, 132.
24 D. R. Richardson, D. S. Kalinowski, V. Richardson, P. C. Sharpe, D. B. Lovejoy, M. Islam and P. V. Bernhardt, *J. Med. Chem.*, 2009, **52**, 1459.
25 J. Chan, A. L. Thompson, M. W. Jones and J. M. Peach, *Inorg. Chim. Acta*, 2010, **363**, 1140.
26 A. Gomez-Hens and M. Valcarcel, *Microchem. J.*, 1984, **29**, 253.
27 G. Gran, *Acta Chem. Scand.*, 1950, **4**, 559.
28 A. Avdeef, K. J. Box, J. E. A. Comer, M. Gilges, M. Hadley, C. Hibbert, W. Patterson and K. Y. Tam, *J. Pharm. Biomed. Anal.*, 1999, **20**, 631.
29 H. M. Irving, M. G. Miles and L. D. Pettit, *Anal. Chim. Acta*, 1967, **38**, 475.
30 *SCQuery, The IUPAC Stability Constants Database*, Academic Software (Version 5.5), Royal Society of Chemistry, 1993–2005.
31 A. Sabatini, A. Vacca and P. Gans, *Talanta*, 1974, **21**, 53.
32 L. Zékány, I. Nagypál, in: *Computational Methods for the Determination of Stability Constants*, ed. D. L. Leggett, Plenum Press, New York, 1985, p. 291.
33 C. F. Baes, R. E. Mesmer, *The Hydrolysis of Cations*, Wiley, New York, 1976.
34 E. Farkas, E. Kozma, T. Kiss, I. Toth and B. Kurzak, *J. Chem. Soc., Dalton Trans.*, 1995, 477.
35 H. Sigel, A. D. Zuberbühler and O. Yamauchi, *Anal. Chim. Acta*, 1991, **255**, 63.
36 J. I. Wirgau, I. Spasojevic, H. Boukhalfa, I. Baticic-Haberle and A. L. Crumbliss, *Inorg. Chem.*, 2002, **41**, 1464.